Important Notice to Authors

No further publication processing will occur until we receive your response to this proof.

Attached is a PDF proof of your forthcoming article in PRA. Your article has 5 pages and the Accession Code is **AT11700**.

Please note that as part of the production process, APS converts all articles, regardless of their original source, into standardized XML that in turn is used to create the PDF and online versions of the article as well as to populate third-party systems such as Portico, Crossref, and Web of Science. We share our authors' high expectations for the fidelity of the conversion into XML and for the accuracy and appearance of the final, formatted PDF. This process works exceptionally well for the vast majority of articles; however, please check carefully all key elements of your PDF proof, particularly any equations or tables.

Figures submitted electronically as separate files containing color appear in color in the online journal. However, all figures will appear as grayscale images in the print journal unless the color figure charges have been paid in advance, in accordance with our policy for color in print (https://journals.aps.org/authors/color-figures-print).

Specific Questions and Comments to Address for This Paper

1 Deleted the word "new" to conform to journal style; please see **http://publish.aps.org/authors/new-novel-policy-physical-review**
2 Spelled out QED at first use in the text. OK as done?
3 Deleted "(a.u)" in Fig. 6. OK as done?
4 Please verify Ref. [13].
FQ: This funding provider could not be uniquely identified during our search of the FundRef registry (or no Contract or Grant number was detected). Please check information and amend if incomplete or incorrect.
Q: This reference could not be uniquely identified due to incomplete information or improper format. Please check all information and amend if applicable.

Open Funder Registry: Information about an article's funding sources is now submitted to Crossref to help you comply with current or future funding agency mandates. Crossref's Open Funder Registry (https://www.crossref.org/services/funder-registry/) is the definitive registry of funding agencies. Please ensure that your acknowledgments include all sources of funding for your article following any requirements of your funding sources. Where possible, please include grant and award ids. Please carefully check the following funder information we have already extracted from your article and ensure its accuracy and completeness:
Ministry of Education (TH)
National Research Foundation (AE), NRF-CRP12-2013-03

Other Items to Check

- Please note that the original manuscript has been converted to XML prior to the creation of the PDF proof, as described above. Please carefully check all key elements of the paper, particularly the equations and tabular data.
- Title: Please check; be mindful that the title may have been changed during the peer-review process.
- Author list: Please make sure all authors are presented, in the appropriate order, and that all names are spelled correctly.
- Please make sure you have inserted a byline footnote containing the email address for the corresponding author, if desired. Please note that this is not inserted automatically by this journal.
- Affiliations: Please check to be sure the institution names are spelled correctly and attributed to the appropriate author(s).
- Receipt date: Please confirm accuracy.
- Acknowledgments: Please be sure to appropriately acknowledge all funding sources.
- Hyphenation: Please note hyphens may have been inserted in word pairs that function as adjectives when they occur before a noun, as in "x-ray diffraction," "4-mm-long gas cell," and "*R*-matrix theory." However, hyphens are deleted from word pairs when they are not used as adjectives before nouns, as in "emission by x rays," "was 4 mm in length," and "the *R* matrix is tested."

  Note also that Physical Review follows U.S. English guidelines in that hyphens are not used after prefixes or before suffixes: superresolution, quasiequilibrium, nanoprecipitates, resonancelike, clockwise.
- Please check that your figures are accurate and sized properly. Make sure all labeling is sufficiently legible. Figure quality in this proof is representative of the quality to be used in the online journal. To achieve manageable file size for online delivery, some compression and downsampling of figures may have occurred. Fine details may have become somewhat fuzzy, especially in color figures. The print journal uses files of higher resolution and therefore details may be sharper in print. Figures to be published in color online will appear in color on these proofs if viewed on a color monitor or printed on a color printer.
- Please check to ensure that reference titles are given as appropriate.
- Overall, please proofread the entire *formatted* article very carefully. The redlined PDF should be used as a guide to see changes that were made during copyediting. However, note that some changes to math and/or layout may not be indicated.

Ways to Respond

- ***Web:*** If you accessed this proof online, follow the instructions on the web page to submit corrections.
- ***Email:*** Send corrections to praproofs@aptaracorp.com
  Subject: **AT11700** proof corrections
- ***Fax:*** Return this proof with corrections to +1.703.791.1217. Write **Attention:** PRA Project Manager and the Article ID, **AT11700**, on the proof copy unless it is already printed on your proof printout.

PHYSICAL REVIEW A **00**, 003800 (2018)

Operating a near-concentric cavity at the last stable resonance

ChiHuan Nguyen,[1] Adrian Nugraha Utama,[1] Nick Lewty,[1] and Christian Kurtsiefer[1,2,*]
[1]*Centre for Quantum Technologies, 3 Science Drive 2, Singapore 117543*
[2]*Department of Physics, National University of Singapore, 2 Science Drive 3, Singapore 117542*

(Received 10 June 2018; published xxxxxx)

Near-concentric optical cavities of spherical mirrors can provide technical advantages over the conventional near-planar cavities in applications requiring strong atom-light interaction, as they concentrate light in a very small region of space. However, such cavities barely support stable optical modes, and thus impose practical challenges. Here, we present an experiment where we maintain a near-concentric cavity at its last resonant length for laser light at 780 nm resonant with an atomic transition. At this point, the spacing of two spherical mirror surfaces is 207(13) nm shorter than the critical concentric point, corresponding to a stability parameter $g = -0.999962(2)$ and a cavity beam waist of 2.4 μm.

DOI: 10.1103/PhysRevA.00.003800

I. INTRODUCTION

Optical cavities are widely used, ranging from lasers and gravitational wave detectors to experiments in quantum physics exploring nonlinear atom-light interaction. In particular, atom-cavity systems with ultrahigh finesse cavities are a key component in demonstrations of quantum logic gates, distributed quantum networks, quantum metrology, and sensing applications using cavity quantum electrodynamics [1–4]. The intricate high-reflectivity coatings of the cavity mirrors used in these experiments, however, can pose a challenge on
1 scaling systems up. Therefore, types of optical cavities and resonance structures that enhance the electrical field of an optical mode have been considered recently [5,6]. One such cavity design that has been experimentally demonstrated is a near-concentric Fabry-Perot cavity [6,7]. Outside the field of
2 cavity quantum electrodynamics (QED), these near-unstable cavities have been considered to reduce the influence of thermal noise of the mirror coatings on gravitational wave detectors [8].

Near-concentric cavities are formed by two spherical mirrors with a normal separation l_{cav} just short of the sum of the two radii of curvatures. In a near-concentric cavity with a length of several millimeters, the effective mode volume can be very small and comparable to state-of-the-art cavities of micrometer lengths due to the tight focusing mode. The relatively large mirror separation permits one to form a cavity with a narrow spectral linewidth already with mirrors of low finesse that are less challenging to make. The ratio of coupling strength over cavity decay rate is proportional to $F\sqrt{l_{\text{cav}}}/w$, which is more favorable for longer cavity lengths at a given cavity finesse F and a cavity mode waist w.

Other advantages are a better optical access to the focal region, which can be helpful for preparation and manipulation of quantum emitters. For use with trapped ions, the large separation between two mirrors provides the ability to avoid charging problems with dielectric surfaces, which has been a major hindrance to the development of ion traps in optical cavities [9]. Furthermore, the near degeneracy in resonant frequencies of transverse modes of near-concentric cavities is an intriguing feature to explore the physics of multimode strong coupling in cavity quantum electrodynamics [10]. However, near-concentric cavities have not been widely explored yet, mainly because they require mirrors that cover a relatively large solid angle, and because of technical hurdles of stabilizing both the longitudinal and transverse mirror positions.

Here, we report on a compact design of a symmetric near-concentric cavity with a length of 11 mm corresponding to a free spectral range of 13.6 GHz, and the strategy to stabilize it to the last few stable resonances near the concentric point. The design is intended to study atom-light interaction but can be easily adapted to a wider range of experiments.

II. OPTICAL SETUP

A. Cavity design

The spherical cavity mirrors of our cavity have a radius of curvature $R_C = 5.5$ mm, and a nominal reflectivity of $R = 99.5\%$ at a wavelength of 780 nm. For effective matching to an external probe mode, we use an ellipsoidal second surface to transform a collimated (Gaussian) input mode into a spherical wave at the mirror surface. The details of characterization and abberations analysis of the mirrors can be found in [11].

To align the cavity and correct for thermal drifts, we place one of the cavity mirrors on a shear piezo stack with a travel range of $\pm 5\,\mu$m in three orthogonal directions. The cavity mounting system is shown in Fig. 1 and fits into a cuvette of a vacuum chamber which provides convenient optical access to the cavity focus for other optical beams preparing atoms in experiment. Except for the cavity mirror shields, all the mechanical parts are made from titanium to reduce the structural change of the mounting system due to thermal fluctuation.

*christian.kurtsiefer@gmail.com

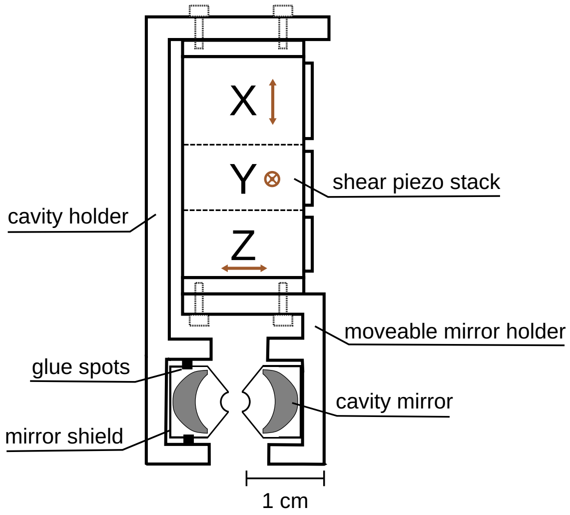

FIG. 1. Schematic of a near-concentric cavity assembly. Arrows indicate the moving directions of piezo segments.

B. Alignment procedure

The relatively large numerical aperture of near-concentric cavity modes and the aspheric outside surface of the cavity mirrors require that the optical axes of the two cavity mirrors coincide—a requirement that is much less critical in conventional cavity arrangements. Additionally, the absolute transverse separation of the mirror surfaces needs to be near the critical distance within the moving range of the piezo translator.

A collimated laser beam between two fiber couplers defines a reference line for the alignment of the cavity mirrors. One cavity mirror is pre-assembled in the movable mirror holder. Then the other cavity mirror is gradually moved into the cavity holder on an external translation stage. Throughout the alignment process, the reflected beams from the two cavity mirrors are monitored and ensured to couple back to the optical fibers. This keeps the tilt of the mirrors under control, and provides a coarse transverse alignment between the two cavity mirrors. The fine adjustment is carried out by a piezo system on the external translation stage, before the mirror is glued into the aligned position inside the cavity holder.

C. Longitudinal locking scheme

As we intend to use the cavity for cavity QED experiments, we need to stabilize its resonance frequency with respect to an atomic transition independently from the light used to interact with the atom-cavity system. Therefore, a separate wavelength, far detuned from the atomic transition under consideration is used. The optical layout of the locking scheme is shown in Fig. 2. Laser light at wavelengths of 780 nm and 810 nm is coupled into the near-concentric cavity, which we refer to as probe and the lock light, respectively. The probe laser is referenced to a D2 transition of ^{87}Rb via a modulation transfer spectroscopy [12]. The stability of the probe laser is passed to the lock laser at 810-nm wavelength via a transfer cavity. For that, the transfer cavity is first locked to the probe laser. Then, one sideband generated by an electro-optical modulator (EOM) on the 810-nm light is locked to a resonance of the transfer cavity. By tuning the frequency of the sideband, the frequency of the lock laser can be adjusted, and is chosen such that the probe and lock beams are simultaneously resonant with the near-concentric cavity. The probe light itself can be tuned around the atomic resonance through

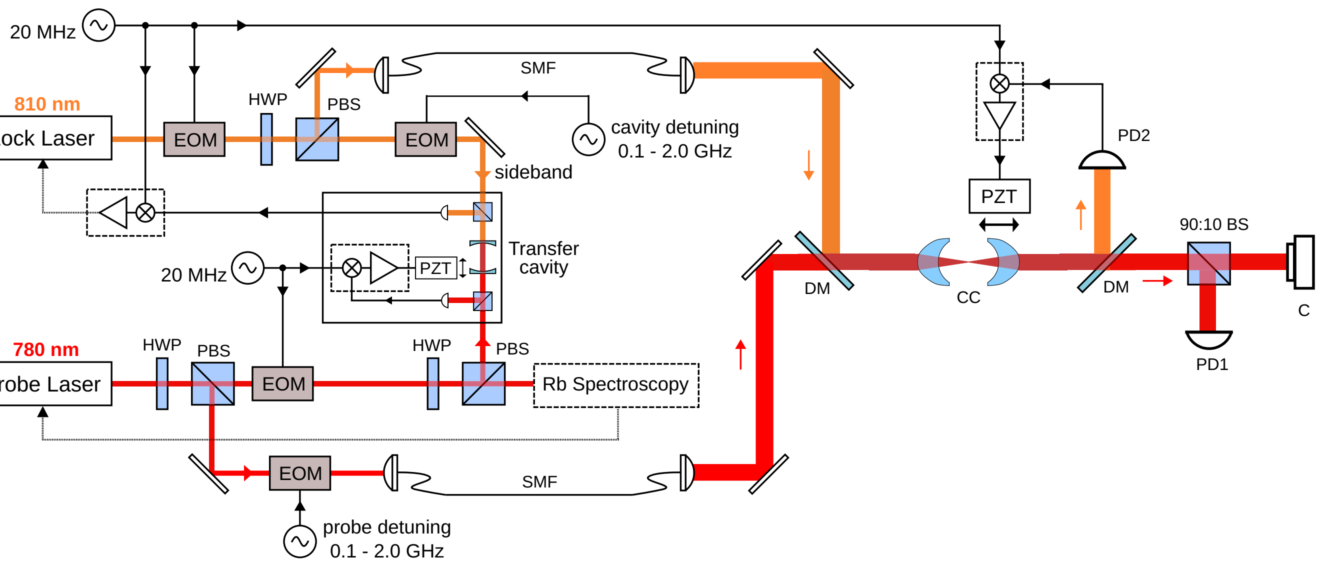

FIG. 2. Locking scheme of the near-concentric cavity setup. Red and orange lines indicate the beams from the 780-nm probe laser and 810-nm lock laser, respectively. The frequency of the probe laser is stabilized to a D2 transition of ^{87}Rb by modulation transfer spectroscopy. The lock laser's sideband is locked to resonance of the transfer cavity, which in turn is stabilized to the probe laser. The frequency of the lock laser can be tuned by adjusting the sideband frequency. The near-concentric cavity is stabilized to the lock laser. All cavity locking schemes use the standard Pound-Drever-Hall technique with 20-MHz phase modulation. The cavity transmission of probe and lock lasers are separated by a dichroic mirror (DM). A camera with linear response (C) and a photodetector (PD1) are placed at the cavity transmission's 780-nm arm to observe the resonant modes. PBS, polarization beam splitter; BS, beam splitter; SMF, single-mode fibers.

another EOM in a similar way. All locks use the standard Pound-Drever-Hall technique [13] with additional sidebands at 20 MHz which never reach the near-concentric cavity.

III. CAVITY LENGTH MEASUREMENT

The eigenmodes of an optical resonator with spherical mirrors can be described by Laguerre-Gaussian (LG) functions, as they form a complete basis to solutions of the paraxial wave equation, and capture well the cylindrical symmetry of the resonator along the optical axis [14]. We denote cavity modes as LG_{nlp} with integer number mode indices n, l, p. Modes of different n identify longitudinal modes, while l and p characterize the transverse mode profile. The resonance frequencies of the cavity modes are fixed by the condition that the round-trip phase shift in the cavity must be an integer multiple of 2π. As the cavity length approaches concentric point, the shift of the transverse mode frequencies approaches the free spectral range. Therefore all transverse modes become co-resonant in the concentric regime.

Making use of this property, we determine the cavity length by measuring the spacing of resonant frequencies between the fundamental mode LG_{00} and the transverse mode LG_{10}. Under paraxial approximation, the resonance frequencies of the cavity with identical spherical mirrors are given by

$$\nu_{n,l,p} = n\frac{c}{2l_{\rm cav}} + (1+|l|+2p)\frac{c}{2l_{\rm cav}}\frac{\Delta\psi}{\pi}, \qquad (1)$$

where c is the speed of light, $\Delta\psi = 2\tan^{-1}(l_{\rm cav}/2z_0)$ the Gouy phase difference after one round trip of LG_{00}, and z_0 the Rayleigh range of the cavity [15]. From Eq. (1) follows an expression for frequency spacing of LG_{00} and LG_{10} in terms of $l_{\rm cav}$ and R_C,

$$\Delta\nu_{\rm tr} = \nu_{n00} - \nu_{n10} = \frac{c}{2l_{\rm cav}}\left(1 - \frac{\cos^{-1} g}{\pi}\right), \qquad (2)$$

where $g = 1 - l_{\rm cav}/R_C$ is the stability parameter.

In the experiment, we obtain cavity transmission spectra by varying the cavity length within a free spectral range.

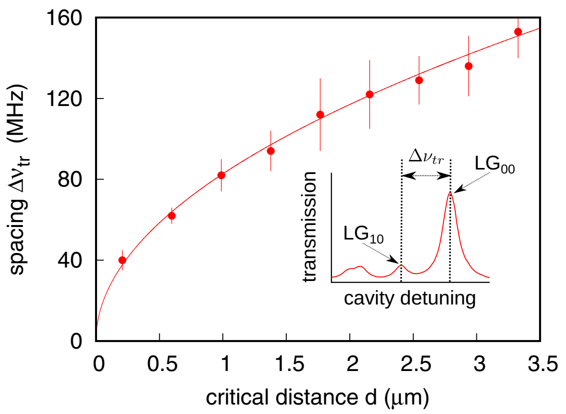

FIG. 3. Transverse-mode frequency spacing ($\Delta\nu_{\rm tr}$) at different critical distance (d) of cavity lengths that are resonant with the 780-nm laser. The solid line is the fit based on Eq. (2). Error bars show the standard deviation of the measurement. The inset shows a typical cavity transmission spectrum and the derived $\Delta\nu_{\rm tr}$.

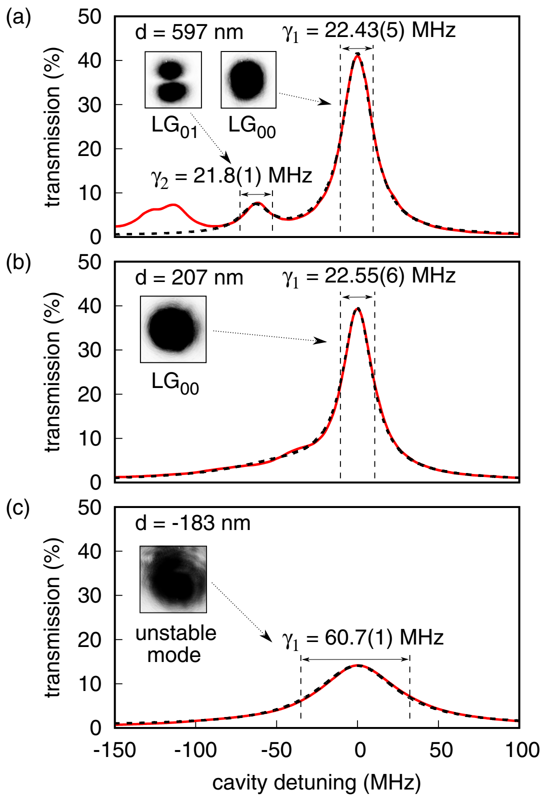

FIG. 4. Cavity transmission spectra, measured by detuning the cavity through small changes (few nm) in the cavity length. (a) $d =$ 597 nm. The dashed line is a fit to a sum of two Lorentzian functions modeling two resonant peaks. (b) $d = 207$ nm. Transverse modes become degenerate and form a long tail extending out to the lower frequencies. (c) $d = -183$ nm. The cavity is in the unstable regime. Insets show the transmitted transverse mode profiles recorded by a (partly saturated) camera.

We record spectra at different resonant cavity lengths, and apply a peak detection algorithm to determine the resonant frequencies. Different transverse modes are distinguished by imaging the intensity distribution of light transmitted through the cavity with a camera. The frequency measurements are calibrated with a frequency marker obtained by modulating the probe laser with an electro-optical phase modulator (EOM).

Figure 3 shows the transverse mode frequency spacing at different cavity lengths which are resonant with the 780-nm laser. We define the critical distance as $d = 2R_C - l_{\rm cav}$. From a fit of experimental data points to Eq. (2), we determine $d =$ 207(13) nm at the last stable resonance, which corresponds to the stability parameter $g = -0.99996(2)$. This is consistent with our observation that when increasing the cavity length by another half wavelength, the cavity enters the unstable regime and exhibits lossy cavity modes (see Fig. 4 and the next section).

The good agreement between the experimental data, including the last resonant point, and the fit based on the paraxial equation prompts us to discuss the validity of the paraxial approximation in our near-concentric cavity. In the paraxial approximation, the complex electric field amplitude of a beam propagating in the z direction can be described as $E(x, y, z) = u(x, y, z)e^{-ikz}$, where k is the longitudinal wave vector component, and $u(x, y, z)$ an envelope function; its slow variation in the paraxial approximation requires

$$\left|\frac{\partial^2 u}{\partial^2 z}\right| \ll \left|2k\frac{\partial u}{\partial z}\right|. \tag{3}$$

Conventionally, Eq. (3) is considered valid for optical beam components with an angle with the optical axis up to ≈30 degrees [16]. Transverse fundamental near-concentric cavity modes (LG_{n00}) have a beam divergence of $\theta = \lambda/\pi w_0$, where λ is the wavelength of the resonant mode (780 nm in our case) and w_0 is the cavity beam waist. Taking the beam divergence now as a characteristic angle with the optical axis, the divergence limit of 30 degrees for the paraxial approximation corresponds to $w_0 \leqslant 496$ nm, or equivalently $d \leqslant 0.5$ nm. The region of critical distances we explore is much larger, so the paraxial approximation is still valid. Note that the definition of the critical distance d and validity of Eq. (1) are based on a meaningful definition of a mirror surface position. The thickness of the dielectric Bragg stacks forming the mirrors for our cavity exceeds by far the critical distances d for the last stable longitudinal resonances, so the absolute position of the mirror surface has to refer to an effective position of these Bragg stacks.

IV. CAVITY MODE ANALYSIS

Earlier observations indicated that the cavity finesse reduces significantly as the cavity is pushed toward the geometrical instability regime [17]. In contrast to this, possibly due to refined manufacturing techniques of large angle spherical mirror surfaces, we find that our near-concentric cavity can maintain the transmission and linewidth at the last two resonant cavity lengths before the unstable regime. Typical cavity transmission spectra are shown in Fig. 4. To characterize linewidths of slightly overlapping cavity modes, we model the cavity transmission by a sum of two Lorentzian functions,

$$T(\nu) = \frac{T_1}{4(\nu-\nu_1)^2/\gamma_1^2+1} + \frac{T_2}{4(\nu-\nu_2)^2/\gamma_2^2+1}, \tag{4}$$

where $T_{1(2)}$ are transmission coefficients, $\nu_{1(2)}$ resonant frequencies, and $\gamma_{1(2)}$ the linewidths of cavity modes LG_{00} and LG_{10}. From a fit of Eq. (4) to cavity transmission spectra we then determine the cavity parameters at multiple cavity lengths.

We find that at $d = 207$ nm, the last longitudinal resonance of the cavity, the fundamental mode maintains the cavity linewidth and transmissions of other longitudinal resonances. The observed linewidth of the fundamental mode LG_{00} infers a cavity finesse of 603 and still agrees well with the nominal value of 21.7 MHz determined from the cavity mirror's design reflectivity of 0.995 at a wavelength of 780 nm. Given the measured cavity length, we obtain a cavity mode waist of 2.44 μm at the cavity center and 0.56 mm at the cavity mirrors. This cavity mode waist is among the tiniest achieved in cavity QED experiments [18]. In contrast, the transverse modes start to overlap at the last resonant length, and the probe laser simultaneously couples to multiple cavity modes such that the second cavity mode becomes difficult to identify, resulting in a broadened effective linewidth of 98(2) MHz from the fit. An increase of the cavity length by another half wavelength leads to a decrease in the cavity transmission and an increase in the cavity linewidth, which are indicative of unstable cavity modes.

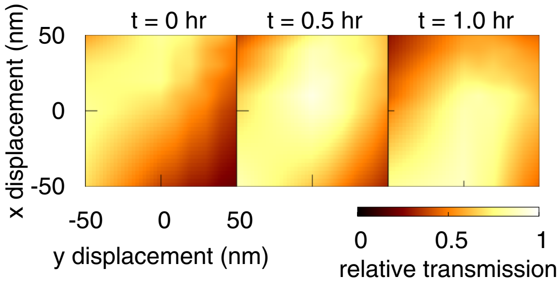

FIG. 5. Drift of cavity alignment. Light transmitted through a cavity resonance is coupled to a single mode fiber as a mode filter. The relative transmission (before and after the single mode fiber) as a function of transverse displacement of the second cavity mirror is shown over some time without any stabilization.

Besides the scattering and absorption loss, due to the finite mirror aperture, the cavity can exhibit additional geometrical diffraction losses if there is misalignment between the two optical axes of the cavity mirrors. This loss becomes more critical for near-unstable cavities. Hence, we try to assess the misalignment in our cavity based on the observed variation of cavity linewidth across the cavity lengths. Under the assumption that the misalignment is entirely due to the tilting of the mirrors, the diffraction loss per round trip is given by [19]

$$\alpha = \theta^2 \frac{1+g^2}{(1-g^2)^{3/2}} \frac{\pi l_{cav}}{\lambda} \frac{(a/w_m)^2}{\exp[2(a/w_m)^2]-1}, \tag{5}$$

where θ is the misalignment angle, a the radius of cavity mirror aperture, and w_m the beam waist on the mirrors. Attributing all cavity losses to such diffraction losses bounds the misalignment to about 0.5 degrees. This is compatible with what we expect from the alignment procedure, as the reflected laser beams from the cavity mirrors are ensured to couple back to the optical fibers.

V. TRANSVERSE STABILIZATION

The alignment of near-concentric cavities is sensitive to the transverse positions of the cavity mirrors. To quantify this, we measure the coupling efficiency of a resonant cavity mode to the mode defined by a single mode fiber as we displace one of the cavity mirrors in x and y directions (see Fig. 5). Throughout the measurement, the cavity length is locked to the frequency stabilized 810-nm laser. The transmission profiles in Fig. 5 show a full width at half maximum (FWHM) of 42(8) nm and 54(10) nm for displacements in x and y. We observe a drift of 22 nm of cavity alignment over a time of 1 h. With the thermal expansion coefficients of the cavity setup, such a change of the fundamental mode transmission by 10% could be caused by a temperature change on the order of 100 mK. Practical operation of a near-concentric cavity therefore requires either careful temperature stabilization of the setup, or a transverse locking scheme. To actively compensate for transverse drifts, we implement a two-dimensional lock-in

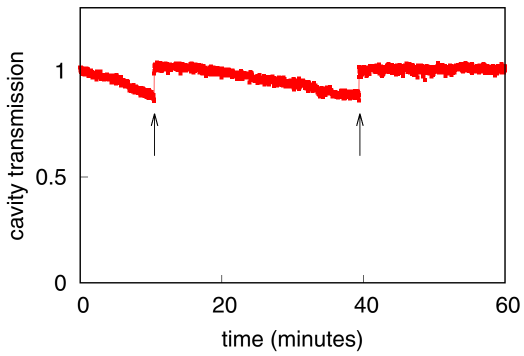

3 FIG. 6. Transverse stability of the near-concentric cavity at the last stable longitudinal resonance ($d = 207$ nm). The slow drift of cavity transmission on the order of minutes is due to the transverse misalignment caused by temperature change, while the cavity length is locked to a probe light resonance during the measurement. Vertical arrows indicate the activation of the stabilization algorithm, where the cavity transmission recovers to the maximum value after the successful implementation of the algorithm within a few seconds.

algorithm based on the gradient search method to maximize the cavity transmission for the two transverse displacement variables. Figure 6 shows a typical record of cavity transmission at the last resonant length when the stabilization algorithm is activated at two instances. The slow drift on the order of minutes between these instances is probably caused by the temperature change of the cavity. The average search time to recover the maximum cavity transmission is on the order of seconds, and thus would not significantly reduce the duty cycle of an experiment. With both temperature stabilization and active transverse stabilization, the near-concentric cavity remains aligned for a few hours.

VI. CONCLUSION

We presented a compact design, alignment procedure, and stabilization methods of a Fabry-Perot near-concentric optical cavity. In our experiment, we find that the cavity design preserves cavity linewidth and cavity transmission when being operated at 207(13) nm shorter than the concentric point, the last longitudinal resonance for this cavity setup.

At this cavity length, the measured transverse mode frequency spacing of 40(5) MHz is of the same order as the estimated atom-cavity coupling strength of 20 MHz for a Rb atom placed into the cavity mode. This permits one to probe the dynamics of an atomic state when strongly coupling to several cavity modes, opening an avenue to experimentally explore the multimode cavity QED in the optical regime, and new schemes of interaction of photons simultaneously present in different modes.

ACKNOWLEDGMENTS

This work was supported by the Ministry of Education in Singapore and the National Research Foundation, Prime Minister's office (partly under Grant No. NRF-CRP12-2013-03). FQ

[1] H. J. Kimble, Phys. Scr. **1998**, 127 (1998).
[2] S. Ritter, C. Nölleke, C. Hahn, A. Reiserer, A. Neuzner, M. Uphoff, M. Mücke, E. Figueroa, J. Bochmann, and G. Rempe, Nature (London) **484**, 195 (2012).
[3] A. Reiserer, N. Kalb, G. Rempe, and S. Ritter, Nature (London) **508**, 237 (2014).
[4] A. Reiserer and G. Rempe, Rev. Mod. Phys. **87**, 1379 (2015).
[5] K. C. Cox, D. H. Meyer, N. A. Schine, F. K. Fatemi, and P. D. Q Kunz, J. Phys. B: At. Mol. Opt. Phys. **51**, 195002 (2018).
[6] C. H. Nguyen, A. N. Utama, N. Lewty, K. Durak, G. Maslennikov, S. Straupe, M. Steiner, and C. Kurtsiefer, Phys. Rev. A **96**, 031802 (2017).
[7] S. E. Morin, C. C. Yu, and T. W. Mossberg, Phys. Rev. Lett. **73**, 1489 (1994).
[8] H. Wang, M. Dovale-Álvarez, C. Collins, D. D. Brown, M. Wang, C. M. Mow-Lowry, S. Han, and A. Freise, Phys. Rev. D **97**, 022001 (2018).
[9] M. Harlander, M. Brownnutt, W. Hänsel, and R. Blatt, New J. Phys. **12**, 093035 (2010).
[10] K. E. Ballantine, B. L. Lev, and J. Keeling, Phys. Rev. Lett. **118**, 045302 (2017).
[11] K. Durak, C. H. Nguyen, V. Leong, S. Straupe, and C. Kurtsiefer, New J. Phys. **16**, 103002 (2014).
[12] D. J. McCarron, S. A. King, and S. L. Cornish, Meas. Sci. Technol. **19**, 105601 (2008).
[13] R. W. P. Drever, J. L. Hall, F. V. Kowalski, J. Hough, G. M. Ford, A. J. Munley, and H. Ward, Appl. Phys. B: Photophys. Laser Chem. **31**, 97 (1983). 4
[14] L. Allen, M. W. Beijersbergen, R. J. C. Spreeuw, and J. P. Woerdman, Phys. Rev. A **45**, 8185 (1992).
[15] B. E. A. Saleh and M. C. Teich, Resonator Optics, in *Fundamentals of Photonics* (John Wiley & Sons, New York, 2001), pp. 310–341.
[16] A. E. Siegman, *Lasers* (University Science Books, South Orange, 1986).
[17] A. Haase, B. Hessmo, and J. Schmiedmayer, Opt. Lett. **31**, 268 (2006).
[18] B. Brandstätter, A. McClung, K. Schüppert, B. Casabone, K. Friebe, A. Stute, P. O. Schmidt, C. Deutsch, J. Reichel, R. Blatt, and T. E. Northup, Rev. Sci. Instrum. **84**, 123104 (2013).
[19] R. Hauck, H. P. Kortz, and H. Weber, Appl. Opt. **19**, 598 (1980).